

Materials with simultaneously negative permittivities and permeabilities are called MTMs. These materials are known not to exist in natural form in materials, were made by composing an array of metallic wire and split ring resonators (SRRs) [5]. A substantial amount of research has been made in different phases for both fundamental electromagnetic and practical applications of these unusual materials in different frequency ranges from radio to optical frequencies. Unusual electromagnetic phenomena of MTMs had been predicted theoretically by Veselago [6] such as reversals of Doppler shift and the Vavilov-Cerenkov effects, perfect lensing, reversal of radiation pressure to radiation tension, and negative refraction. All of these phenomena are direct results of the group velocity inversion of electromagnetic waves propagating in such media. For this reason, Veselago named the MTMs as left handed material (LH). The structure of MTMs consists of an array of nonmagnetic conduction SRRs that have negative permeability combined with plasmonic wires that exhibit negative permittivity [7].

One of the first observations of the LH nature of the MTMs structures was inferred by observing transmission and reflection coefficients over a broad band of frequency. For the separate geometries (rods only or SRRs only), no transmission occurs because of an imaginary wave number. In the frequency band where the two parameters are simultaneously negative, transmission occurs by considering the combined geometry. This band-pass phenomenon was indeed observed in the MTMs [8].

However, this transmission is not enough to deduce that the material reveals LH behavior. A more thorough test to demonstrate the LH nature of a material is required either by directly measure the phase inside the material or to measure the index of refraction of a prism. Snell's law states that the angle of transmission into or out of any right-handed (RH, with positive permittivity and permeability) material must be on the opposite side of the surface normal with respect to the incident angle. For LH materials, however, the angle of transmission is on the same side of the normal, which has been theoretically demonstrated and experimentally verified [6, 8].

Moss et al. [9] have studied MTMs in certain frequency bands using three-dimensional Finite Difference Techniques (FDT). The study showed that fields propagating inside the MTM with forward power direction exhibit a backward phase velocity and negative index of refraction.

Dolling et al. [10] have studied the properties of the femtosecond laser pulse propagating through MTMs that has negative index of refraction for waves around 1.5 μm . Kim et al. [11] have studied the guided dispersion characteristics of grounded MTMs slab waveguides. The results show that

Double-Negative Metamaterial Optical waveguide Behavior Subjected to Stress

superslow waves, backward waves, and mode suppressions can be obtained in certain circumstances, which cannot occur in conventional grounded dielectric slab.

Stress effect on the behavior of the waveguide has been observed in photoelectric devices. Stress can cause anisotropic and inhomogeneous distribution of the refractive index. Huang [12] has studied the stress effect on the performance of symmetrical optical waveguides consists of dielectric surrounded by dielectric cladding and core. He showed that different stress states can affect the central wavelength and effective index which degrade the performance of the waveguide.

Stress effect on the performance of an asymmetric waveguide sensor consists of dielectric slab sandwiched between nonlinear cladding and linear substrate is performed by El-Khozondar et. al. [13]. The result of this study showed that the stress affects the performance of the sensor by changing the effective index and the central wavelength. El-Khozondar et. al. [14] extended this study to understand the behavior of a symmetrical waveguide sensor consists of dielectric slab surrounded by nonlinear media subjected to stress. Results show that careful choosing of loading method and materials can control the performance of the sensor.

The focus of this study is on understanding the effect of stress on the performance of the waveguide sensor. The proposed structure of the sensor consists of dielectric slab inserted between cladding and substrate made of MTMs. The dispersion equation of the proposed structure is analytically derived for both TE and TM modes. The effective index as a function of different stress is plotted using Maple algorithms. The effect of stress is investigated using various values of the MTMs parameters keeping the value of $\epsilon\mu = 4$. The plan of this study is as follows; section 2 is dedicated to understand the structure of the waveguide sensor and the field equations. Hydrostatic stress effect on the optical behavior of the waveguide is introduced in section 3. Section 4 focuses on the effect of in-plane stress on the optical performance of the waveguide sensor. The next section gives final conclusion.

2. Planar Waveguide Structure

The structure of the waveguide sensor consists of a dielectric core surrounded by MTMs as shown in Fig. 1. The core is assumed to have a thickness of the order of the wavelength and higher refractive index than the surroundings cladding and substrate. The light is confined in x direction and propagates in the z-direction. It is assumed that the fields have no variation in the y direction. Although, most practical waveguides are also confined in the y direction, planar waveguide are used to provide a basic

understanding since analytical solution may be obtained for this kind of structure. The core media is anisotropic and inhomogeneous having a dielectric tensor (ϵ) depends on the value of stress. The structure of the waveguide is considered symmetric; therefore, the material constants of the cladding and the substrate are identical, i.e. $\epsilon_c = \epsilon_s = \epsilon_1$ and $\mu_c = \mu_s = \mu_1$.

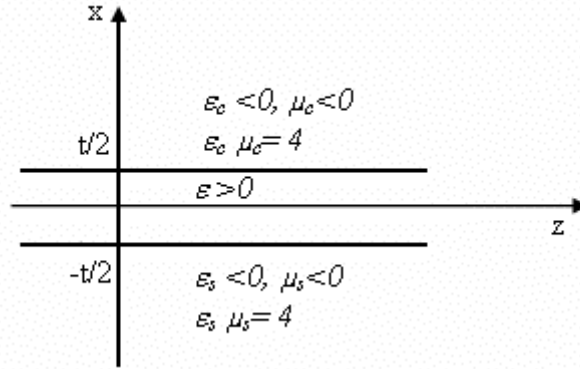


Fig. 1: The structure of the planar waveguide sensor

The waveguide is very long in the z direction. Therefore, the shear stresses in the z direction can be ignored which simplify the dielectric tensor (ϵ) to

$$\epsilon = \begin{pmatrix} n_{xx}^2 & n_{xy}^2 & 0 \\ n_{xy}^2 & n_{yy}^2 & 0 \\ 0 & 0 & n_{zz}^2 \end{pmatrix}. \quad (1)$$

where n_{xx} , n_{yy} , n_{zz} , and n_{xy} depends of the stress values^[12]. The TE, $E_z=0$, and TM, $H_z=0$, mode equations at the core, $-t/2 \leq x \leq t/2$, are derived from Maxwell equations as follows,

$$\text{TE: } \frac{d^2 e_y}{dx^2} + k^2 \left(n_{yy}^2 - n_e^2 - \frac{n_{xy}^4}{n_{xx}^2 - n_e^2} \right) e_y = 0, \quad (2)$$

$$\text{TM: } \frac{d^2 h_y}{dx^2} + p \frac{dh_y}{dx} + k^2 \frac{n_{zz}^2}{n_{xx}^2} \left(n_{xx}^2 - n_h^2 - \frac{n_{xy}^4}{n_{yy}^2 - n_h^2} \right) h_y = 0, \quad (3)$$

Double-Negative Metamaterial Optical waveguide Behavior Subjected to Stress

where $p(x) = \frac{-2}{n_{zz}} \frac{dn_{zz}}{dx}$, n_e and n_h are the effective index for TE and

TM respectively, and k is the propagation constant in vacuum. For simplicity the stress effect in the surrounding media is ignored. Therefore, the mode equation at the surrounding, $x \leq -t/2$ for substrate and $x \geq t/2$ for cladding, is expressed as

$$\frac{d^2 e_y}{dx^2} - k^2 (n_e^2 - \mu_i \varepsilon_i) e_y = 0, \quad (4)$$

where $\mu_i < 0$ and $\varepsilon_i < 0$ with $\mu_i \varepsilon_i = 4$, and $i = c$ and s for cladding and substrate respectively.

3. Hydrostatic stress:

It is assumed that the core is only affected by hydrostatic stress, i.e., $\sigma_{xx} = \sigma_{yy} = \sigma_{zz} = \sigma$ and $\sigma_{xy} = 0$. Therefore, the core refractive index varies with stress as follow

$$n_{xx} = n_{yy} = n_{zz} = n = n_0 - (C_1 + 2C_2)\sigma, \quad (5)$$

where C_1 and C_2 are stress-optics constants^[15]. Consequently, the mode equations for TE (2) and for TM (3) of the core are simplified to

$$\text{TE: } \frac{d^2 e_y}{dx^2} + k^2 (n^2 - n_e^2) e_y = 0, \quad (6)$$

$$\text{TM: } \frac{d^2 h_y}{dx^2} + k^2 (n^2 - n_h^2) h_y = 0, \quad (7)$$

By using the boundary condition of zero fields at infinity, the dispersion equation for both TE and TM can be solved, and the solutions are listed in table 1.

Table 1: Solution for TE and TM modes under hydrostatic stress state

| Region | TE solutions | TM solutions |
|---------------|---|---|
| $x \geq t/2$ | $A_E \exp(-kx \sqrt{n_e^2 - n_1^2})$ | $A_M \exp(-kx \sqrt{n_h^2 - n_1^2})$ |
| $t/2 > x $ | $B_E \cos(kx \sqrt{n^2 - n_e^2}) + C_E \sin(kx \sqrt{n^2 - n_e^2})$ | $B_M \cos(kx \sqrt{n^2 - n_h^2}) + C_M \sin(kx \sqrt{n^2 - n_h^2})$ |
| $-t/2 \geq x$ | $D_E \exp(kx \sqrt{n_e^2 - n_1^2})$ | $D_M \exp(kx \sqrt{n_h^2 - n_1^2})$ |

Where A, B, C, D are constants can be found from boundary conditions. At the interface between core and surroundings, the boundary conditions are: e_y and h_z are continuous for TE, and h_y and e_z are continuous for TM. Applying boundary conditions yields dispersion equations which are listed in table 2.

Table 2: Transverse equations for TE and TM modes under hydrostatic stress state

| TE modes | TM modes |
|--|--|
| $P \tan\left(\frac{kt}{2} P\right) = \frac{q}{\mu_1}$; even | $P \tan\left(\frac{kt}{2} P\right) = \frac{qn^2}{\varepsilon_1}$; even |
| $\frac{q}{\mu_1} \tan\left(\frac{kt}{2} p\right) = -P$; odd | $q \tan\left(\frac{kt}{2} p\right) = -\frac{\varepsilon_1}{n^2} P$; odd |

Where $P = \sqrt{n^2 - n_i^2}$ and $q = \sqrt{n_i^2 - \mu_1 \varepsilon_1}$, n_i is the effective refractive index where i represent e or h for TE and TM respectively; t is the core thickness; and n is the dielectric refractive index of the core as defined in equation (5).

The effective refractive index is drawn as a function of the core thickness under different states of hydrostatic stress for both TE (Fig. 2 (a)) and TM (Fig. 2 (b)). For MTMs, cladding and substrate, two cases are considered: case one the values of the ε_1 and μ_1 are -8 and -0.5 respectively, and case two the values of the ε_1 and μ_1 are -5 and -0.8. For both cases, the stress is assumed to take two states -0.01 and 0.01. One of the well-known dispersion characteristics of conventional dielectric slab waveguide is that the cutoff of the principle mode ($m=0$) does not exist, which means that the mode can propagate, regardless of how thin the slab thickness is. In our structure, this cutoff is absent as shown in Fig. 2 (a) and Fig. 2 (b). The figures exhibit the effect of the stress on the cutoff of the allowed modes. For example, consider the TE case, with slab thickness has the value $t = 1 \mu\text{m}$, $\varepsilon_1 = -8$ and $\mu_1 = -0.5$ subjected to stress equals -0.01, zero mode ($m=0$)

Double-Negative Metamaterial Optical waveguide Behavior Subjected to Stress

and first mode ($m=1$) will appear as shown in Fig. 2 (a). While when the stress value equals 0.01 only $m=0$ will appear. In the case of TM, only $m=0$ is propagating at $t=1\mu\text{m}$. Fig. 3 shows the effective refractive index as a function of stress for core thickness has value, $t=1\mu\text{m}$ for TE (a) and TM (b). For TE, both $m=0$ and $m=1$ appears for low values of stress and $m=1$ disappears at higher stress values.

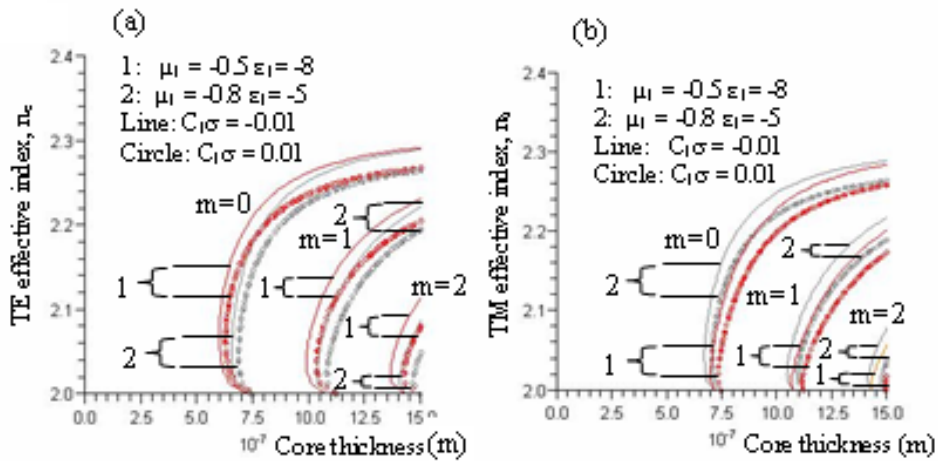


Fig. 2: The effective refractive index versus the core thickness under different hydrostatic stresses. (a) TE. (b) TM

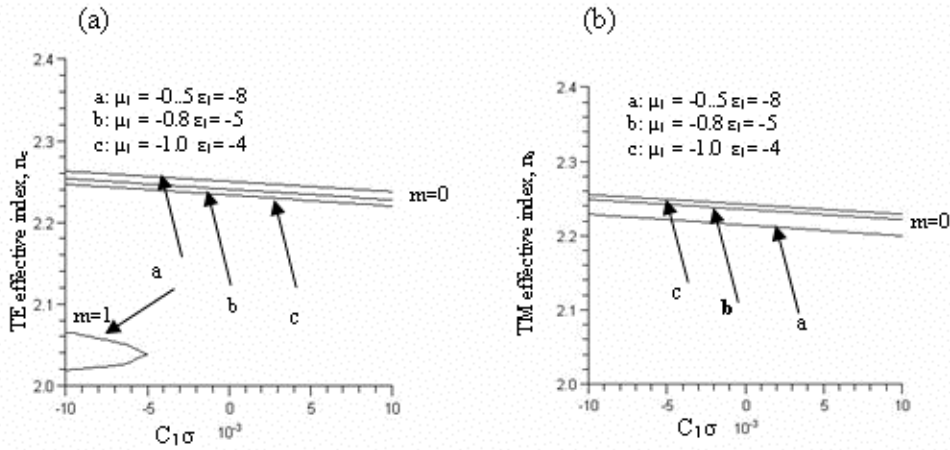


Fig. 3: The effective refractive index as a function of hydrostatic stress for core thickness $t=1\mu\text{m}$. (a) TE. (b) TM

It is shown that the stress can affect the behavior of the waveguide. Consequently, by controlling the size of the waveguide we can control the number of modes under certain stress state.

4. In-plane stress state:

It is assumed that the core is only affected by in-plane stress, i.e., $\sigma_{xx} = 0$, $\sigma_{xy} = 0$, and $\sigma_{yy} = \sigma_{zz} = \sigma$. The effective index in the core [12] is expressed as follows,

$$\begin{pmatrix} n_{xx} \\ n_{yy} \\ n_{zz} \end{pmatrix} = \begin{pmatrix} n_0 - 2C_2\sigma \\ n_0 - (C_1 + C_2)\sigma \\ n_0 - (C_1 + C_2)\sigma \end{pmatrix}. \quad (8)$$

The core mode equations (2) and (3), are simplified to

$$\text{TE: } \frac{d^2 e_y}{dx^2} + k^2 (n_{yy}^2 - n_e^2) e_y = 0, \quad (9)$$

$$\text{TM: } \frac{d^2 h_y}{dx^2} + k^2 (n_{zz}^2 - n_{zz}^2 n_h^2 / n_{xx}^2) h_y = 0, \quad (10)$$

Applying the same boundary conditions as in hydrostatic state, the above equations have solutions shown in table 3. Also, the dispersion equation for both TE and TM are listed in table 4.

Table 3: Solution for TE and TM modes under in-plane stress state

| Region | TE solutions | TM solutions |
|---------------|---|---|
| $x \geq t/2$ | $A_E \exp\left(-kx \sqrt{n_e^2 - n_1^2}\right)$ | $A_M \exp\left(-kx \sqrt{n_{zz}^2 n_h^2 / n_{xx}^2 - n_1^2}\right)$ |
| $t/2 > x $ | $B_E \cos\left(kx \sqrt{n_{yy}^2 - n_e^2}\right) + C_E \sin\left(kx \sqrt{n_{yy}^2 - n_e^2}\right)$ | $B_M \cos\left(kx \sqrt{n_{zz}^2 - n_{zz}^2 n_h^2 / n_{xx}^2}\right) + C_M \sin\left(kx \sqrt{n_{zz}^2 - n_{zz}^2 n_h^2 / n_{xx}^2}\right)$ |
| $-t/2 \geq x$ | $D_E \exp\left(kx \sqrt{n_e^2 - n_1^2}\right)$ | $D_M \exp\left(kx \sqrt{n_{zz}^2 n_h^2 / n_{xx}^2 - n_1^2}\right)$ |

Double-Negative Metamaterial Optical waveguide Behavior Subjected to Stress

Table 4: Transverse equations for TE and TM modes under in-plane stress state

| TE modes | TM modes |
|--|--|
| $P \tan\left(\frac{kt}{2}P\right) = \frac{q}{\mu_1}; \text{ even}$ | $P \tan\left(\frac{kt}{2}P\right) = \frac{n_{zz}^2 q}{\epsilon_1}; \text{ even}$ |
| $\frac{q}{\mu_1} \tan\left(\frac{kt}{2}P\right) = -P; \text{ odd}$ | $q \tan\left(\frac{kt}{2}P\right) = -\frac{\epsilon_1 P}{n_{zz}^2}; \text{ odd}$ |

where

$$P = \begin{cases} \sqrt{n_{yy}^2 - n_e^2} & \text{for TE} \\ \sqrt{n_{zz}^2 - n_{zz}^2 n_h^2 / n_{xx}^2} & \text{for TM} \end{cases}, \quad (11)$$

$$q = \begin{cases} \sqrt{n_e^2 - \mu_1 \epsilon_1} & \text{for TE} \\ \sqrt{n_{zz}^2 n_h^2 / n_{xx}^2 - \mu_1 \epsilon_1} & \text{for TM} \end{cases}. \quad (12)$$

The effective refractive index is drawn as a function of the core thickness under different states of in-plane stresses for both TE (Fig. 4 (a)) and TM (Fig. 4 (b)). Fig. 5 shows the effective refractive index for TE as a function of stress for core thickness of value, $t=1\mu\text{m}$.

Fig. 4 and Fig. 5 demonstrate that stress can affect the performance of the waveguide sensor, i.e. modes may appear or disappear depending on the value of stress which might induce multimode effect. In addition, a cutoff zero modes at which no propagation might occur

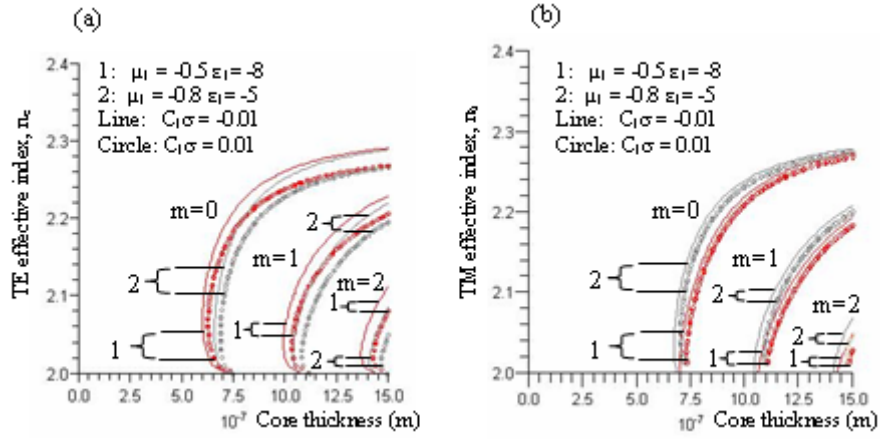


Fig. 4: The effective refractive index versus the core thickness under different in-plane stresses. **(a)** TE. **(b)** TM

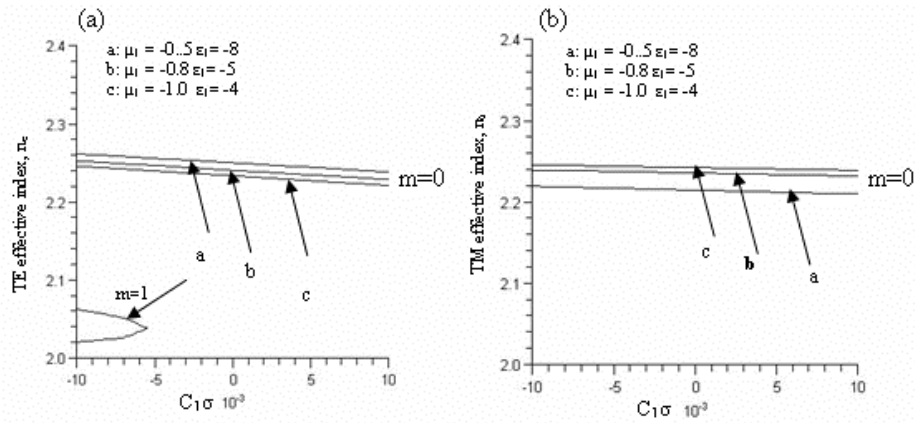


Fig. 5: The effective refractive index as a function of in-plane stress for core thickness $t=1\mu\text{m}$. **(a)** TE. **(b)** TM

Conclusion

This work demonstrates the behavior of MTMs in a symmetric waveguide sensor. The three-layered waveguide sensor is a dielectric sandwiched between MTMs cladding and substrate. Results show that stress can control the behavior of the sensor and might cause multimode effect. Stress affects the value of the cutoff for each mode. The value of effective index varies with stress state values. Therefore, the results of this study are valuable to manufacturers and help them to take into consideration the stress effect on the optical performance during processing and fabrication.

References:

1. Lukosz, W., "Integrated optical chemical and direct biochemical sensors", *Sensors Actuators B* **29**, 37–50 (1995).
2. Kunz, R. E. Miniature integrated optical modules for chemical and biochemical sensing *Sensors Actuators B* **38**, 13–28 (1997).
3. Voros, J., Ramsden, J. J., Csucs, G., Szendro, I., De Paul, S. M., Textor, M., and Spencer, N. D., "Optical grating coupler biosensors", *Biomaterials* **23**, 3699–710 (2002).
4. Horva' th, R., Pedersen, H. C., Larsen, N. B., "Demonstration of reverse symmetry waveguide sensing in aqueous solutions", *Appl. Phys. Lett.* **81** (12), 2166-2168 (2002)
5. Smith, D. R., Padilla, W. J., Vier, D. C., Nemat-Nasser, S. C., and Schultz, S., "Composite medium with simultaneously negative permeability and permittivity ", *Phys. Rev. Lett.* **84** (18), 4184 (2000).
6. Veselago, V. G., "The electrodynamics of substances with simultaneously negative values of ϵ and μ ", *Soviet Physics* **10** (4), 509 (1968).
7. Yoon, J., Song, S. H., Oh, C., and Kim, P. , "Backpropagating modes of surface polaritons on a cross-negative interface", *Optics Express* **13** (2), 417 (2005).
8. Shelby, R. A., Smith, D. R., and Schultz, S., "Experimental verification of a negative index of refraction", *Science* **292** , 77 (2001).
9. Moss, C. D., Grzegorzczuk, T. M., Zhang, Y., and Kong, J. A., "Numerical studies of left handed metamaterials", *Progress In Electromagnetics Research* **PIER 35**, 315 (2002).
10. Dolling, G., Enkrich, C., Wegener, M., Soukoulis, C. M., Linden, S., "Simultaneous Negative Phase and Group Velocity of Light in a Metamaterial", *Science* **312**, 892 (2006).
11. Kim, K. Y., Cho, Y. K., and Tae, H., "Guided Modes Propagations of Grounded Double-Positive and Double-Negative Metamaterial Slabs

- with Arbitrary Material Indexes", *Journal of the Korean Physical Society* **49**, 577 (2006).
12. Huang, M., "Stress effect on performance of optical waveguides", *International Journal of Solids and Structures* **40**, 1615 (2003).
 13. El-Khozondar, H.J., El-Khozondar, R. J., Shabat, M. M., Koch, A.W., "Stress Effect on Optical Nonlinear Waveguide Sensor", *Journal of Optical Communications* (2006, in press).
 14. El-Khozondar, H. J., Shabat, M. M., Abu Tair, G., and Abadla, M., "Thermal Stress effects on nonlinear thin film Waveguide Sensors", *Ukraine journal of physics and chemistry of SOLID STATE* **8 (2)** (2007, in press).
 15. Xu, J., Stroud, R., *Acousto-optic Devices: Principles, Design, and Applications*. New York: John Wiley and Sons (1992).